From geological interpretation and 3D modelling to the characterization of the deep seated EGS reservoir of Soultz (France).

Sausse J. *, Dezayes C. **, Genter, A. **

* UMR CNRS 7566 G2R, Nancy Université, BP 239, 54506 Vandoeuvre lès Nancy cedex, France; ** BRGM, Geothermal Energy Department, BP 36009, 45060 Orléans Cedex 2, France.

judith.sausse@g2r.uhp-nancy.fr

Keywords: 3D fracture network, reservoir characterization, Soultz-sous-Forêts.

ABSTRACT

This study presents a 3D interpretation of the geophysical logs run after the drill of three wells at 5 km depth in the framework of the Soultz European EGS (Enhanced Geothermal Systems) project. The major fracture zones encountered in these wells are characterized through examination of borehole image logs, classical geophysical well logs and cutting samples. In the open holes of the granite massif, the flow logs and temperature profiles allow to distinguish natural flowing fractures. These large-scale fracture zones are characterized by sealed core and an around damage zone that is highly fractured and therefore highly permeable. The fractures are identified and measured in orientation and in dip by borehole imagery techniques. The major issue for reconstructing the 3D geometry of the Soultz fracture network is the question of the fracture extension. In a first approach, we define and correlate the fracture extensions according to the importance of flow observed on flow log runs during the injection and stimulation tests in the wells. A maximal fracture extension of 600 m length is proposed, excepted for the most important fault zone that extends to 2000 m. This geometry seems to be in agreement with the development of microseismicity within these fracture planes during the 1997-2003 hydraulic stimulation phases at Soultz. The model is enclosed in a 3D regular grid. The grid axes fit on the directions of the maximal anisotropy of the microseismic cloud (N170°E). The main fractures are modeled by planar discs centered on the wells respecting the fracture orientations and widths. Moreover, each plane is characterized by a property corresponding to its permeability assumed as proportional to the importance of the flow developed in the vicinity of the fracture zones. Storage capacities and types of permeability are quantified. They are similar for the production wells but strongly different for the injection well. The 3D well connectivity is modeled and discussed. This geological model could be used as a geometrical basis for fracture quantification of fracture porosity and permeability in the EGS reservoir.

1. INTRODUCTION

Soultz-sous-Forêts, located in the Upper Rhine Graben, hosts one of the few deep geothermal 'Enhanced Geothermal System' test sites in the world. At its current state of development, the EGS site consists of three boreholes: GPK2, GPK3 and GPK4, the European geothermal pilot plant which extends to more than 5000 m depth, GPK1 a first hydraulic test well which extends to 3600 m and a reference hole EPS1 which has been fully cored down to 2230 m (Figure 1).
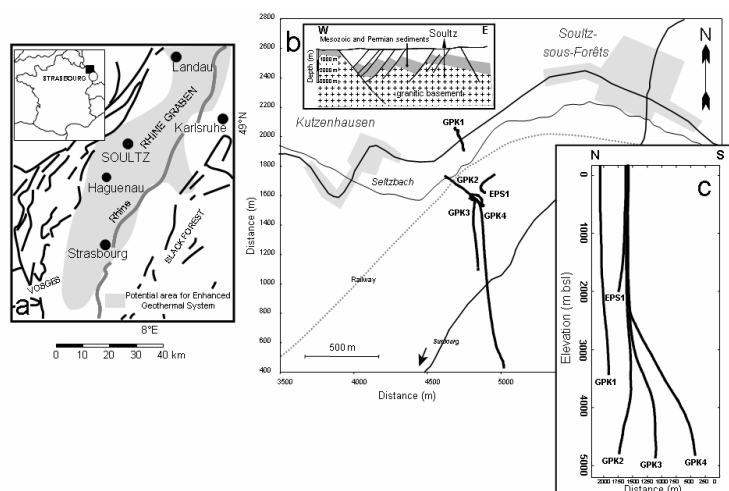

Figure 1: Schematic geological map of the Rhine Graben and location of the Soultz-sous-Forêts EGS site (a and b). Location and traces of the Soultz deep geothermal wells; solid lines correspond to well traces (b and c). (Modified after Dezayes et al., 1995, 2005).

In deep enhanced geothermal systems (EGS), natural or forced fluid circulation takes place through the fracture networks in crystalline rocks characterized by low matrix porosity. The connection between fractures and the consequent anisotropic permeability are then crucial to insure the efficiency of the geothermal exchanger and to recover sufficient fluid temperatures at surface. Wide fractures correspond to zones where large fluid losses occurred during the injection tests at Soultz and often match with thick altered fractured zones. The objective of this paper is therefore an attempt to reconstruct and quantify a 3D network of connected, permeable fractures within the target rock volume between the wells and to achieve a better understanding and prediction of the hydraulic response of the granite. An important database of borehole image logs, classical geophysical well logs and cutting samples (Dezayes et al., 2005) is used to reconstruct the 3D model of the fractured reservoir.

2. GEOLOGICAL AND GEOPHYSICAL SETTINGS

The Soultz granite is a Hercynian monzogranite characterized by phenocrystals of alkali feldspars in a matrix of quartz, plagioclase, biotite and minor amphibole. The granitic basement at Soultz has been strongly altered by flowing fluids (vein and pervasive alterations). Fluid circulation takes place through two fracture networks that create scale-related flow: the first is a closely-connected network of small-aperture fractures that may represent the far-field reservoir, and the second is a set of local, wide-aperture fractures that result in an anisotropic permeability

system connecting the injection and production wells hydraulically (Sausse and Genter, 2005). This hierarchy of flow is strongly dependent on the petrophysical properties of the rock and is directly linked to the intensity of the granite hydrothermal alteration (Sardini et al., 1997; Ledésert et al., 1999; Sausse, 2002; Géraud et al., 2005; Sausse and Genter, 2005; Hooijkaas et al., 2006).

BRGM collected geological and well logging data to characterize the Soultz fractured granite reservoir in terms of petrography, hydrothermal alteration and natural fracture network; well data were acquired by the Schlumberger and Geoservice companies. The main well logging in the three deepest wells (GPK2, GPK3 and GPK4) data consisted of the gamma-ray spectral log. Fracture geometrical properties and their spatial relationships were analyzed based on amplitude and transit time anomalies derived from acoustic image logs (Ultrasonic Borehole Imager; UBI). The fractures can be identified with high accuracy and measured in orientation and in dip by these borehole imagery techniques. Other flow and/or temperature logs were run in the different deep wells during injection and production tests since 2003 and some interpretation of the main fracture and permeable zones are described by Dezayes et al. (2005). These flowing fractures could correspond to isolated fracture, series of thin parallel fractures and large-scale fracture zone. These large-scale fracture zones could be 10 m thickness and are characterized by sealed core and a peripheral damage zone (Figure 2) that is highly fractured and therefore highly permeable. A typical fracture zone corresponds to a quartz vein core with high porosity walls (mean value 9.75%). The main mineral transformations during hydrothermal alterations are illite, chlorite and corrensite (Figure 2, Genter et al., 2000, Evans et al., 2005).
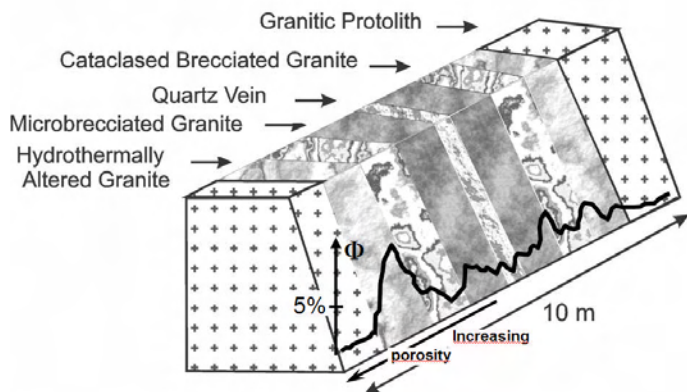

Figure 2: Conceptual lithofacies granite zonation of hydrothermally altered and fractured zone in the Soultz granite and Porosity profile, modified after Genter et al., (2000).

Geometrical and hydraulic parameters such as fracture orientations, their relative contribution to flow are available in the open holes (Figure 3, Table 1) for the three deepest wells (Dezayes et al., 2005).
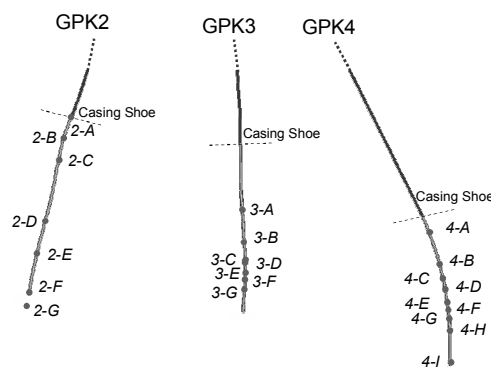

Figure 3: GPK2, GPK3 and GPK4 well trajectories in the deepest part of the reservoir and intersections of the main fracture zones with the well paths in the open hole sections. 7 fracture zones are measured in GPK2 and GPK3 and 9 in GPK4.

3. CONSTRUCTION OF THE 3D MODEL:

3.1. Fracture orientations

The main fractures are modeled by planar discs centered on the wells and respecting the fracture orientations (Table 1). Most of the fractures appear to be members of a nearly-vertical conjugated fracture set with a symmetry axis striking NNE-SSW consistent with the Rhine Graben tectonics. For the GPK2 well, UBI logs were not available, therefore the fracture orientations were fully estimated based from our expertise from the Soultz site.

3.2. Fracture extensions

The major issue for reconstructing the 3D geometry of the Soultz fracture network is the question of the fracture extensions. In a first approach, we define and correlate the fracture extensions according to the importance of flow observed on flow log runs during the injection and stimulation tests in the wells. Fractures are imported from specific gOcad data files that compile all the geometrical properties presented in Table 1. Extension are variable, fixed with an arbitrary correlation between the fracture disc object diameter and the importance of flow registered on flow logs. For example, Figure 4 presents an example of two big fractures zones in GPK2, at 4780 and 4885 m depth, where the flow log indicate fluid losses of around 24%. Extensions of the fracture in the model were weighted by this ratio of fluid losses observed in the different flow logs. Maximal extensions are fixed at 100, 200, 500, 1000, 1500 and 2000 m that correspond to the maximal diameters of the modeled fractures (discs).

Moreover, these maximal extensions are fixed in order to respect one unique criterion: a fracture plane that cuts one well cannot intersect the others if no information indicates the presence of such fracture zone on the UBI images. Therefore, 100, 200, 300, 400, 500 and 600 m were tested in the model and respect this criterion. Higher extensions imply connections between fractures and wells that are not practically observed.
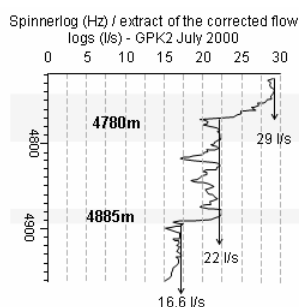
Figure 4: Two fracture zones in GPK2 at 4780 and 4885 measured depth detected on a July 2000 flow log. Fluid losses of 24% each time are measured in front of the fractures.

		classification of the importance of flow	logging depth	dip direction	dip	extension (m)	aperture (m)
GPK2	2-A	7	4440	250	70	86	0.086
	2-B	4	4510	70	70	150	0.150
	2-C	2	4580	70	70	300	0.300
	2-D	1	4780	250	65	600	0.600
	2-E	2	4885	250	65	300	0.300
	2-F	5	5010	250	70	120	0.120
	2-G	6	5050	250	70	100	0.100
GPK3	3-A	1	4775	234	64	*2000*	0.600
	3-B	4	4875	57	78	150	0.150
	3-C	6	4931	262	74	100	0.100
	3-D	7	4940	263	71	86	0.086
	3-E	3	4972	47	72	200	0.200
	3-F	5	4990	270	79	120	0.120
	3-G	2	5025	292	66	300	0.300
GPK4	4-A	7	4823	271	80	86	0.086
	4-B	7	4924	279	73	86	0.086
	4-C	7	4973	269	77	86	0.086
	4-D	7	5010	256	85	86	0.086
	4-E	1	5050	78	74	600	0.600
	4-F	7	5073	61	63	86	0.086
	4-G	7	5100	252	71	86	0.086
	4-H	7	5135	275	67	86	0.086
	4-I	7	5237	288	75	86	0.086

Table 1: Geometrical and hydraulic parameters characterizing the main fracture zones in GPK2, GPK3 and GPK4. The final extension of fracture zone 3-A is determined with several criteria (see text for details).

However, the presence of kilometric fault is well known in the Soultz Graben site. Indeed, one of the fracture zones was specifically treated and was assumed to be the most important in the reservoir. Fracture zone 3-A (Table 1) cuts the well GPK3 at 4775 m depth. A simple extrapolation of the plane orientation was tested to check its intersection with the other wells. After this step, three main observations were surprisingly coincident in the 3D model. First, the fracture plane 3-A cuts GPK2 above the open hole section at 4143 m measured depth. This depth is well known at Soultz because it corresponds to the presence of a huge cave (diameter higher than the caliper 20' arms) and to a casing leak. The casing is broken and a shearing phenomenon was detected at this depth. Such a zone could correspond to the passage of an important fracture zone. Moreover, this fracture zone doesn't cut the well GPK4. The fracture plane 3-A is located around 90 m below the bottom of the hole. Tracer tests performed between 2000 and 2005 in the Soultz wells (Sanjuan et al., 2006) demonstrate that 2 types of circulation are developed between the wells. These tests gave evidence of a fast and relatively direct hydraulic connection between GPK3 and GPK2 (short loop) but also indicated the existence of another larger and slower hydraulic connection between GPK3 and GPK4 (large loop). The absence of direct connection between the open hole of GPK4 and the major fracture zone 3-A could explain these two types of hydraulic behaviors. Finally, the extrapolation of the fracture zone 3-A shows that GPK1, one of the first exploration wells at Soultz, is not intersected. The fracture plane is located at around 300 m below the bottom hole (vertical distance). This gap matches very well with the fault interpretations done during the 1993 VSP (Vertical Seismic Profile) survey performed in the Soultz wells (Cornet et Scotti, 1993, Place et al., 2006, 2007a, 2007b). Indeed, this survey shows that a fracture is well marked on the seismic section, below GPK1 and with a 55°W dip orientation. This fracture could correspond to fracture zone 3-A that is striking N144°E and dipping 64° W. The difference of only 9° between the two dip values could be negligible and is not significant if we keep in mind that the orientation of fracture 3A is derived from UBI interpretation and characteristic of a tight section of the well and that the extrapolation of the fracture plane 3-A reaches a final extension of 2000 m (Table 1).

All these observations could be simple coincidences. However, the assumption that fracture zone 3-A is the main huge structure in the Soultz deep reservoir was done and its extension was fixed to 2000 m. The other fracture plane extensions are limited to a maximal value of 600 m and match with the importance of fluid losses observed during the hydraulic tests as it is previously mentioned.

3.3. Fracture apertures

Then, the fracture apertures are fixed proportionally to the extensions with a ratio of 1000. By this way, minimal values of apertures ranging between 8 cm and of 60 cm are computed (Table 1). Fracture zone 3-A is characterized by the same aperture than the other important hydraulic zones (rank 1 such as fracture zones 2-D and 4-E, Table 1). This ratio between fracture extension and aperture gives only a hierarchy of relative apertures that do not match with the actual widths of the fracture zone i.e. the large zone of alteration halo surrounding the fracture zone itself (until 10 m, Figure 2). Fracture aperture is assumed to be the effective aperture available for fluid flow i.e. that fix the fracture real conductivity.

3. EXPLOITATION OF THE 3D MODEL.

3.1. Microseismicity and 3D fault network

The model is enclosed in a 1 000 000 cells, 3D regular grid extending between 4000 and 5190 m true vertical depth. The grid axes fit on the directions of the maximal anisotropy of the microseismic cloud observed during the different stimulation tests. The grid is aligned with a global N170°E direction and represents a total volume of $5\ 10^9\ m^3$. The vertical and horizontal resolutions are respectively 12 m and 5 m.

The final geometry of the fracture network seems to be in agreement with the development of the microseismicity observed at Soultz during the last 1997-2003 injection phases. This period concerns only the stimulations of GPK2 and GPK3 and consequently, the trajectory of these two well paths were only superimposed to the microseismic cloud presented in Figure 5. A cluster analysis of the microseismic event locations shows that several isolated clusters exist and match with the main fracture connections. Fracture intersections correspond to highly cataclased and altered zones and are therefore potential high permeability

zones. A main continuous body of events fits quite well with one of the biggest fracture plane (2-D) observed at 4780 m depth in GPK2.
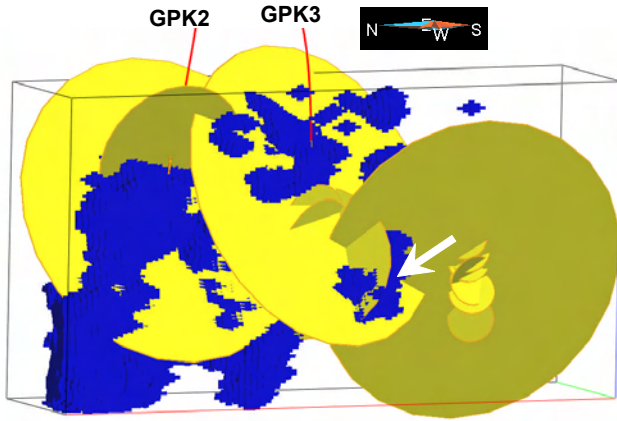

Figure 5: comparison of the location of the microseismic events (blue cells) after a cluster analysis and the 3D fracture network. Main clusters of seismicity could correspond to probable zones where fractures are shearing during the hydraulic stimulations. Clusters of events frequently match with the fracture intersection zones (example with the white arrow).

3.2. Connectivity analysis

The connectivity between the fracture planes is computed and connectivity curves are drawn using connection points within fracture planes and edges, identified to "pipes", that link connected fractures (Macé, 2004 and 2006). The connectivity curves identify main probable fluid flow pathways between GPK2 and GPK3 and GPK3 and GPK4.

The injection well GPK3 shows a cluster of connected fractures centered on 4950 m measured depth and that covers an interval of depth between 4875m and 5025 m around the well trajectory (Figure 6). One of the production well, GPK2, shows less clustering of connected points and two levels of depth are distinguished. A first isolated zone of connection is observed at 4580 m and a second one at 4785 m depth where connections are more clustered. The direct pipe observed around 4580 m bridges directly GPK3 at 4770 m. However, a single cluster of connected points, a potential fluid entry at 4785 m, generates 3 distinct pipes that distribute 3 fluid pathways in the main clustered zone of GPK3 around 4950 m. On another way, GPK3, the injection well, could spread widely fluids towards one single depth point of GPK2. The connections observed in GPK2 are located at higher depths than in GPK3. The storage capacity of fractures in the vicinity of GPK2 is lower than in GPK3 where numerous contact points between fracture planes form an obvious cluster. This cluster is characterized by a large lateral development in the same direction than the main fracture zone (3-A) of GPK3. This big fracture seems to totally control the fluid pathways in the vicinity of the well and at these depths. The storage capacity around 4950 m depth in GPK3 represents a volume of $1.135.10^6$ m^3 compared to $0.925.10^6$ m^3 for the two zones previously described in GPK2 (1.2 times lower than GPK3). GPK4 is connected to GPK3 at a lower depth (5020 m) with a potential storage capacity limited to $0.170.10^6$ m^3 (5.4 times lower than GPK2 and 6.7 times lower than GPK3).

The main connection between the three wells is mainly guided by the most important fracture zone (3.A) that cuts GPK3 at 4775 m. The flow is probably oriented by this fracture plane and goes directly up to reach GPK2 with two distinct pathways. On the contrary the injected fluid goes down to reach GPK4 by two main pathways that connect a tighter zone of depth in GPK4 (around 5020 m). This result could be important to estimate the maximal temperatures reached by the produced fluids in the two production wells GPK2 and GPK4 and therefore crucial for the geothermal exchanger efficiency.
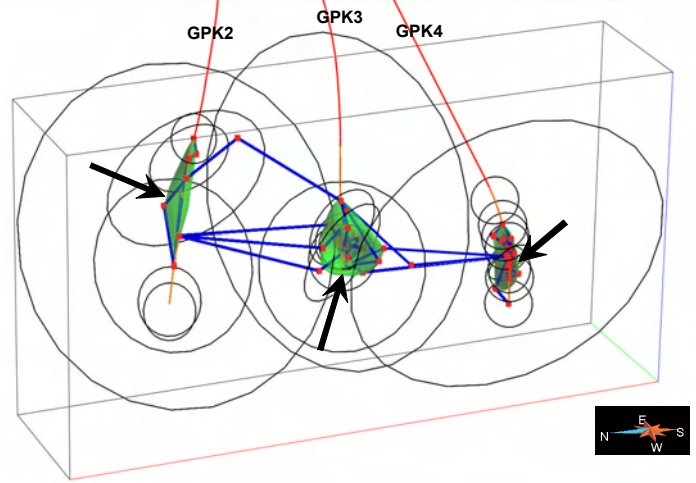

Figure 6: Traces of the fracture plane perimeters (black circles) and main connection curves calculated for the fracture network. Red dots correspond to the centers of intersection zones and blue lines are the shortest connection pathways between the connected fracture planes. The small green envelops centered on the well paths (black arrows) correspond to the potential storage capacities in the vicinity of the different wells.

3.3. 3D fracture conductivity

Fracture equivalent conductivity was estimated using the model proposed by Snow, 1969; Oda, 1986; Ababou, 1991; Vuillod, 1995 and Sausse et al., 1998. This approach proposes to quantify equivalent hydraulic properties on the basis of the geometric parameters of fractures (mainly apertures and spacings). Two assumptions are done with 1) a Poiseuille law to model the flow in each individual fracture assumed to be an infinite plane at the scale of the well and 2) the assumption of a global and homogeneous pressure gradient in the reservoir.

The following equation is proposed:

$$K_i = \frac{g}{12\,h}\,\frac{A_i}{S_i} \qquad (1)$$

Where g is acceleration due to gravity [9,81 m.s^{-2}]., $?$, the kinematic viscosity of the fluid [water: 1. 10^{-6} m^2.s^{-1}], A_i, the fracture i width [m] and S_i, the mean spacing between fracture i and fractures i-1 and i+1 [m].

Vertical spacings are calculated between the fracture plane points in the whole grid. This 1D calculation was performed in each column of the grid and the results displayed in the 3D model with the objective to map relation between fracture aperture and their spacing through the whole reservoir. Each fracture plane is characterized by a constant aperture mentioned in Table 1.

The calculation gives minimal and maximal values of fracture conductivity between $3.2.10^{-12}$ and $1.5.10^{-8}$ m.s^{-1}. Three main modal values are observed at 1.10^{-10}, 5.10^{-10} and 1.10^{-9} m.s^{-1} whereas only 10% of the grid cells support conductivities higher than $2.5.10^{-9}$ m.s^{-1} (black bars on the frequency histogram, Figure 7).
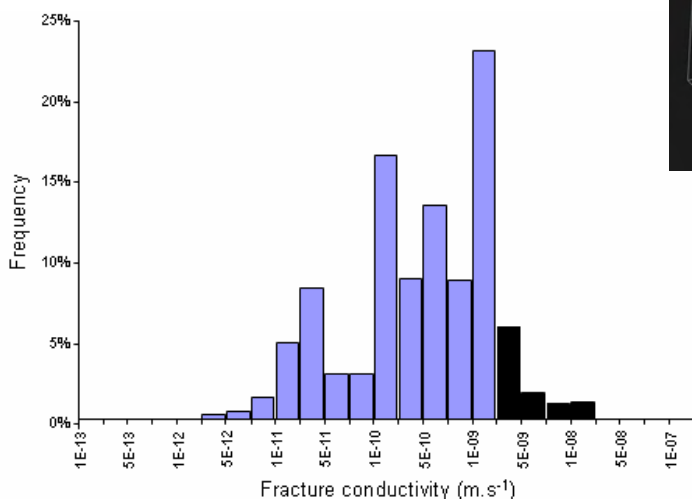

Figure 7: Frequency histogram showing the distribution of fracture conductivities calculated in function of fracture apertures and spacings. The black bars of the histogram describe the highest conductivity values.

In such crystalline rocks, where the matrix porosity and permeability are low, the 3D distribution of fracture conductivity figures the potential distribution of the reservoir permeability. In the grid, the previous conclusions concerning connection of the fracture planes stay reliable because spacings and connectivity are logically linked. Zones of high fracture conductivity match with zones where high connection degree is observed (Figures 6 and 8). The important storage capacity zone around GPK3 is described again by its important volume distribution and by permeability values mainly higher than 5.10^{-9} m.s^{-1}.

The volume of rock where non null values of conductivity are observed represents $1.93.10^{8}$ m^{3}, i.e. 3.88 % of the grid model. In this volume, the zones where clusters of fractures intersect correspond to the damage and cataclased zones where conductivities higher than 2.10^{-9} m.s^{-1} are calculated. These high porosity zones represents a volume of $7.77.10^{5}$ m^{3} (0.40% of the fracture porosity) and therefore an effective porosity for fluid flow.
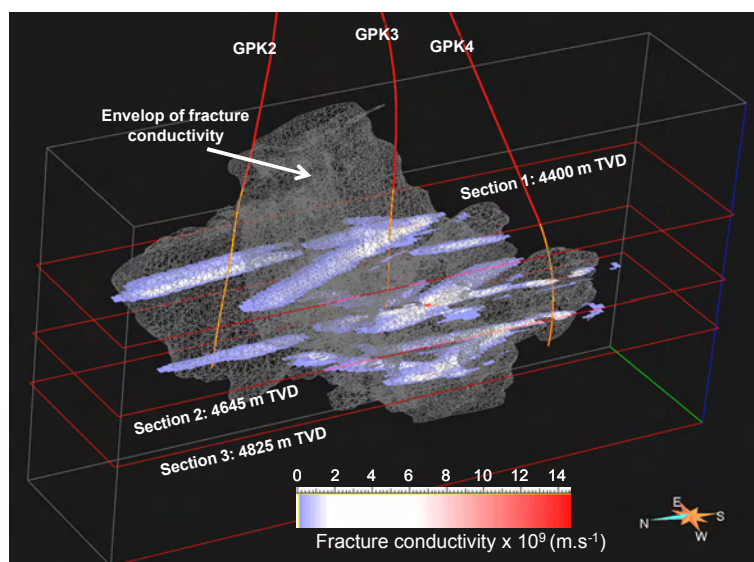

Figure 8: 3D fracture conductivity mapped on three sections of the grid: 4400, 4645 and 4825 m TVD. These sections illustrate the connections between GPK2 and GPK3 at a higher level of depth than the connection between GPK3 and GPK4. The grey mesh superimposed represents the surface envelop limiting no data and existing data values of conductivity.

4. DISCUSSION

Discontinuities such as fractures are potential sites for fluid circulation and have important implications for the hydraulic properties of rocks. The matrix permeability of igneous rocks is generally small and, consequently, the global permeability is mostly controlled by the fracture and crack networks. Therefore, the quantification of the fractured rock hydraulic properties strongly depends on the knowledge of the geometrical parameters of fractures (orientation, extension, aperture, density). However, even if the orientation of fractures can be measured by field observations or borehole imagery, many problems appear when the quantification of their extensions and apertures is considered.

The extension parameter is essential when the probability of fracture intersections (percolation threshold) is calculated. However, the length of a fracture can be measured only if its two lateral ends are visible. In the Soultz reservoir and in many other cases, this is not possible. The only criterion stays to respect the fact that fractures are precisely located by UBI on the well paths and cannot artificially appear because of too large extrapolations of their extension. Some correlation studies could be done (Valley and Evans, 2007 and personal communication) to try to match fractures from well to well but this exercise is complex and not always relevant. The matching between microseismicity and fracture extension is used in this paper to fit a limit of the fracture extensions. However, the 3D relocation of micro earthquakes is done with error bars of around 20 to 30 m (Charléty et al., 2005) and the real influence of the fluid on the generation of large seismic event is still misunderstood and debatable. However Charléty et al. (2005) identifies an obvious correlation between the apparition and location of the microseismic events and the existence of the fracture zone 3-A described by Dezayes et al. 2005.

A fracture is usually defined as two smooth and parallel planes separated by a constant hydraulic aperture. This

Sausse J., Dezayes C., Genter, A.

approach is generally used in the case of regular fracture networks with smooth and widely open fractures. In this case, the fracture permeability corresponds to global and often maximal conductivities controlled by the cubic law. However, in the case of the Soultz fracture zones, where clusters of thin, hydrothermally altered conjugated fissures and fractures intersect each other to produce a highly cataclased zone, the choice of realistic values of apertures is therefore complex. A solution could come from statistical laws describing the fracture geometry and linking the extensions to the fracture apertures. These statistical laws could be evaluated and tested on outcrops of analog rocks in the future (Place et al., 2006, 2007a and 2007b). In this paper, this work has not been done and the choice of a simple ratio between extension and fracture is assumed.

The recent VSP survey (April 2007) performed at Soultz in the deep wells will probably help us to improve the 3D model of the deep fracture zones developed within the Soultz EGS reservoir.

5. CONCLUSION

A 3D interpretation of the geophysical logs run after the drilling of the three deep Soultz wells at 5 km is presented. The different geometrical parameters (orientation, extension, apertures) of the fracture zones are discussed. A maximal extension of 600 m length (disc diameter in the model) is proposed for the highest permeable fracture zone except for the most important fault zone (3-A) that extends to 2000 m. This geometry seems to be in agreement with the development of microseismicity within the 1997-2003 hydraulic stimulations. Storage capacities and types of permeability are described. They are similar for the two production wells GPK2 and GPK4 that are however strongly different of the permeable environment of the injection well GPK3. This well is controlled by a main fracture zone (3-A) and is characterized by an anisotropic important storage capacity. GPK2 and GPK4 show a tighter fracture porosity distribution in the vicinity of localized potential production points. The connection between GPK2 and GPK3 is controlled by one fracture zone (3-A). However, the connection between GPK3 and GPK4 is not linked to this major structure but is relayed by the biggest fracture zone observed in GPK4 that bridges less developed structures of GPK3.

This geological model could evolved with time with the integration of the future VSP data but can be used now as a geometrical basis for the quantification of fracture porosity and permeability in the EGS reservoir.

6. ACKNOWLEDGEMENTS:

REFERENCES

Ababou, R., Approaches to large scale unsaturated flow in heterogeneous stratified and fractured geologic media. Section 4.2: Hydraulic properties of saturated fractured media, *Report*, NUREG/CR-5743, U.S. Nuclear Regulatory Commission, Washington, (1991).

Charléty, J., Cuenot, N., Dorbath, C., and Dorbath, L., Four dimensional velocity structure of the Soultz sous-Forêts geothermal reservoir during the 2000 and 2003 stimulations, P*roceedings*, Thirtieth Workshop on Geothermal Reservoir Engineering, Stanford University, Stanford, California, January 31-February 2 (2005).

Cornet, F.H., and Scotti, O., Analysis of induced seismicity for fault zone identification, *Int. J. Rock Mech. Min. Sci. & Geomech. Abst.*, **30**, (1993), 789-795.

Dezayes, C., Villemin T., Genter, A., Traineau, H., and Angelier, J., Analysis of Fractures in Boreholes of Hot Dry Rock Project at Soultz-sous-Forêts (Rhine Graben, France), *Journal of Scientific Drilling*, **5** (1), (1995), 31-41.

Dezayes, C., Chevremont, P., Tourlière, B., Homeier, G., and Genter, A., Geological study of the GPK4 HFR borehole and correlation with the GPK3 borehole (Soultz-sous-Forêts, France) - Final Report, *Report BRGM Orléans, France*, **RP-53697-FR**, (2005).

Evans, K. F., Genter, A., and Sausse, J., Permeability creation and damage due to massive fluid injections into granite at 3.5 Km at Soultz: Part 1 - borehole observations, *Journal of Geophysical Research*, **110** (B04203), (2005), 0-19.

Géraud, Y., Surma, F., and Rosener, M., Porosity network of Soultz-sous-Forêts granite: the importance of the damaged zone around fault and fractures. *Proceedings, EHDRA Scientific Conference*, March 17-18, Soultz-sous-Forêts, France (2005).

Genter, A., Traineau, H., Ledésert, B., Bourgine, B., and Gentier, S., Over 10 years of geological investigations within the HDR Soultz project, France. *Proceedings, World Geothermal Congress 2000*, Kyushu-Tohoku, Japan (2000).

Hooijkaas, G.R., Genter, A., and Dezayes, C., Deep-seated geology of the granite intrusions at the Soultz EGS site based on data from 5 km-deep boreholes, Geothermics **35** (5-6), (2006), 484-506.

Ledésert, B., Berger, G., Meunier, A., Genter, A., and Bouchet, A., Diagenetic-type reactions related to hydrothermal alteration in the Soultz-sous-Forêts granite, *European Journal of Mineralogy*, **11**, (1999), 731-741.

Macé, L., Caractérisation et modélisation numériques tridimensionnelles de réservoirs naturellement fractures, *PhD thesis*, Institut National Polytechnique de Lorraine, nancy, France, (2006), 152 p.

Macé, L., Souche, L. and Mallet, J.L., 3D Fracture Modeling Integrating Geomechanics and Geologic Data, *Proceedings*, AAPG International Conference: October 24-27, Cancun, Mexico (2004).

Oda, M., An equivalent continuum model for coupled stress and fluid flow analysis in jointed rock masses, *Water Ressources Research*, **22**, (1986), 1845-1856.

Place, J., Géraud, Y., and Diraison, M., Research of an analogue of the Soultz-sous-Forêts granite in Catalunia. *Proceedings*: ENGINE Workshop1, Defining, exploring, imaging and assessing reservoirs for potential heat exchange, November 6-8, Potsdam, Germany, (2006).

Place, J., Naville, C., and Gérard, A., Test of VSP efficiency for the recognition of highly dipping faults in a deep granitic basement, *report*, EEIG "Heat Mining" Report #01/2007, (2007a).

Place, J., Le Garzic, E., Géraud, Y., and Diraison, M., Preliminary results from fracturation analysis on an analogue granitic batholith and "direct broadcast" of the VSP acquisition at Soultz sous-Forêts geothermal site. *Proceedings*: ENGINE Workshop 2 "Exploring high temperature reservoirs: new challenges for geothermal energy", April 1-4, Volterra, Italy (2007b).

Sardini, P., Ledésert, B., and Touchard, G., Quantification of microscopic porous networks by image analysis and measurements of permeability in the Soultz-sous-Forêts granite (Alsace, France). In: Jamtveit, B. & Yardley, B. (Eds), *Fluid flow and transport in rocks - Mechanisms and effects*, Chapman &Hall, **10**, (1997), 171-188.

Snow, D. T., Anisotropic permeability of fractured media, *Water Resources Research*, **5**, (1969), 1273-1289.

Sausse, J., Genter, A., Leroy, J.L., and Lespinasse, M., Altération filonienne et pervasive: Quantification des perméabilités fissurales dans le granite de Soultz sous Forêts (Bas-Rhin, France), *Bulletin de la Société Géologique de France*, **169** (5), (1998), 655-664.

Sausse, J., Hydromechanical Properties and Alteration of Natural Fracture Surfaces in the Soultz granite (Bas-Rhin, France), *Tectonophysics*, 348, (2002), 169-185.

Sausse, J., and Genter, A., Types of fracture permeability in granite, *Special Publication of the Geological Society of London* (Harvey, P. K., Brewer, T. S., Pezard, P. A. & Petrov, V. A. (eds), **240,** (2005), 1-14.

Valley, B., and Evans, K. F., Stress state at Soultz sous-Forêts to 5 km depth from wellbore, *Proceedings, Thirty-Second Workshop on Geothermal Reservoir Engineering*, Stanford University, Stanford, California, January 22-24 (2007).

Vuillod, E., Modélisation Thermo-Hydro-Mécanique de massifs rocheux fractures, *PhD thesis*, Institut National Polytechnique de Lorraine, Nancy, France, (1995), 216 p.